EXPERIMENTAL INVESTIGATION OF EVAPORATION ENHANCEMENT FOR WATER DROPLET CONTAINING SOLID PARTICLES IN FLAMING COMBUSTION AREA

by

*Dmitrii O. GLUSHKOV, Genii V. KUZNETSOV, Pavel A. STRIZHAK *, and Roman S. VOLKOV*

National Research Tomsk Polytechnic University, Tomsk, Russia

The experimental study of integral characteristics of extinguishing liquid (water) droplet evaporation in flaming combustion area has been held. Optical methods of two-phase and heterogeneous mixtures diagnostics (Particle Image Velocimetry and Interferometric Particle Imaging) have been used for heat and mass transfer process investigation. It was established that small-size solid particles, for example carbon particles in droplet structure can enhance water evaporation in flame area. It was shown that the rate of evaporation process depends on concentration and sizes of solid particles in a water droplet. The correlations have been determined between the sizes of solid particles and water droplets for maximum efficiency of fire extinguishing. The physical aspects of the problem have been discussed.

Key words: *water droplet, evaporation enhancement, solid particles, flame, particle image velocimetry, interferometric particle imaging*

Introduction

In recent years, several directions of technologies application have been developed for influence on flames. The influence on flames is implemented by *finely atomized* water or fine compositions on water basis at fire-fighting and fire source suppressions. For example, offices, apartments, industrial buildings, facilities, and special constructions [1-8], space vehicles and stations [9-11], forests and plantations [12, 13] are considered. Theoretical [14-18] and experimental [19-27] investigations have shown that the application of liquid flows, sprayed in a special way (in particular, the *vapor-droplet cloud*, *steam curtain*, *vapor-water fog*), can significantly increase the efficiency of extinguishing substance use in the flame zone. Minimizing expenses with increasing efficiency effect on flames occurs due to involvement of several impacts. For example, it can be lowering the temperature in the combustion zone at evaporation and movement of liquid drops, as well as repression of oxidant and combustion products by water vapor. The maximum water droplet sizes have been determined, at which intense vaporization can be achieved in a flame combustion area [14-27]. Besides droplets pulverization, preliminary water heating, and reducing typical salt admixtures concentration has been considered as factors which enhance the extinguishing liquid loss in weight and vapor injection in the flame

---

* Corresponding author; e-mail: pavelspa@tpu.ru

132

Glushkov, D. O., *et al.*: Experimental Investigation of Evaporation Enhancement for ...
THERMAL SCIENCE: Year 2016, Vol. 20, No. 1, pp. 131-141

area [24-27]. However, such procedures are not always feasible in actual fire fighting [28-31], especially during large forest fire suppressions by firefighting aircraft [32-34].

One of the factors that significantly affect the extinguishing area evaporation intensity is its composition. This follows from the analysis of macroscopic regularities of evaporation during the motion of liquid droplets through the flames [14-27]. Up to the present, no influence mechanism has been installed of solid particles with different sizes and their concentrations in water on the evaporation rate. The experimental investigation of the process is crucial for firefighting technology development of flammable liquids [35-37] and forest fuel [32-34].

The purpose of present study is the experimental analysis of solid particles in the water droplet structure on evaporation enhancement in the flame area.

Experimental set-up and methods

The experimental set-up (fig. 1) was used for investigation of water droplet evaporation in the high-temperature gas area. The optical particle image velocimetry (PIV) [38-41] and interferometric particle imaging (IPI) [42-44] methods of two-phase and heterogeneous gas-vapor-droplet mixtures diagnostics were used for analysis characteristics of heat and mass transfer processes.
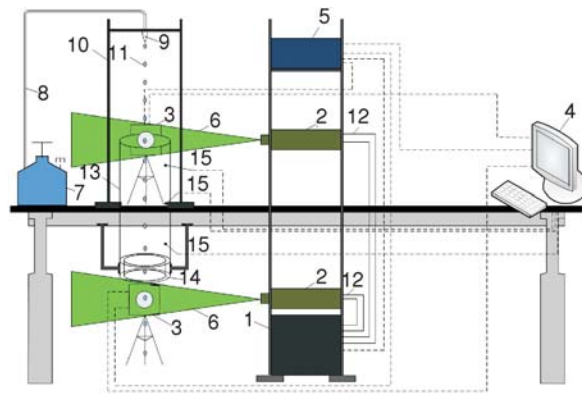

Figure 1. A scheme of experimental set-up
1 – laser generator, 2 – solid state lasers for ultrashort pulses, 3 – cross-correlation digital camera, 4 – personal computer, 5 – synchronizer of personal computer, cross-correlation digital camera, and solid state lasers, 6 – light pulse, 7 – vessel with experimental liquid, 8 – channel of experimental liquid supply, 9 – dosing device, 10 – mount, 11 – droplets, 12 – cooling liquid channel of laser, 13 – cylinder from a heat-resistant translucent material, 14 – hollow cylinder with combustible liquid in internal medium, 15 – thermocouples

The experimental set-up (fig. 1) on the basic elements is similar to that one used in the experiments [24-27]. It includes: cross-correlation digital camera (3) with figure format – 2048×2048 pixels, frame frequency – not less than 1.5 Hz, delay between two sequence figures – not more than 5 ms, double pulsed solid-state laser (2) with an active area of *yttrium aluminum garnet* and neodymium additives which has the wave-length – 532 nm, energy in impulse – not less than 70 mJ, impulse time – not more than 12 ns, recurrence frequency – not more than 15 Hz; synchronizing processor (5) with signal sampling – not more than 10 ns.

The routine of experiments included following procedures. The hollow cylinder (14) (height 0.1 m, diameter of the inner and outer wall are 0.1 m and 0.18 m, correspondingly) was placed at the base of translucent

heat-resistant cylindrical channel (13) (height 1 m, diameter 0.2 m). The flammable with non-fading properties liquid (kerosene) was poured in the internal cylinder medium (14). The flammable liquid ignition was initiated before the experiments beginning. The flame and the high-temperature gas products flow were formed during the kerosene combustion in the inner space of cylindrical channel (13) as a consequence. The liquid was supplied to the dosing device inlet (9) through the channel (8) after warming of internal cylinder hollow (13) to the temperature about 1100 K. The temperature of combustion products was 1070 ± 30 K due to stationary

kerosene combustion while ensuring continuous oxidizer supply. A series of experiments have been conducted over short time intervals (no more than two minutes) to ensure satisfactory repeatability of experiments as in [25-27]. The necessary parameters of liquid outflow (in particular, initial droplet sizes were assumed in a range from 1-5 mm) were exhibited. The lead-in of droplets in a field of high-temperature combustion products channel (13) was realized by the dosing device (9). Illumination of droplet movement trajectory was done by the light pulse (6) of the laser (2). The video recording procedure was carried out by the cross-correlation digital camera (3). Video frames were processed to the personal computer (4). Maximum droplet diameters were calculated and average values of R_d were determined. Water droplet size changes were fixed during the motion through high-temperature gas area. Droplet mass decrease assessments during evaporation in high-temperature gas flow were carried out similar to experimental procedures [24-27].

In the experiments a specialized group of nozzles (tips) for the dosing device (9) has been used. The experiments have been performed with single droplets (*i. e.* in each experiment all the measurements were carried out for only one droplet). The frequency of droplets emission in all the experiments was set constant and equal to six droplets per minute. By changing tips, the sizes of the emitted droplets were changing. The dispenser has been set so that droplets move along the symmetry axis of the cylindrical channel (13) at equal distance from its walls.

Water with small-size (50-500 µm) solid non-metallic (carbon) particles in the structure was used in experiments. The relative mass concentration γ_C of carbon particles in water droplets were varied in a range of 0-1%. Titanium dioxide nanopowder particles were added into the water too. It was used for increasing of water droplet contrast in videogram. The relative mass concentration of titanium dioxide nanopowder was about 0.5%. According to previous studies [24] it was established that nanopowder particles not to dissolve in water and the influence of nanopowder particles on evaporation characteristics could be ignored.

Experiments were carried out in two stages. During the first stage the influence of carbon particles size in water droplet structure was evaluated on its evaporation during droplet motion through the high-temperature gas area. It was used three samples containing particles with different sizes: L_m = 50-70 µm, L_m = 250-300 µm, and L_m = 450-500 µm. Droplet sizes (R_d) changes during its motion through the high-temperature gas area were fixed. During the second stage the influence of carbon particles concentration in water droplet on process enhancement was studied.

The parameter of ΔR was used for numerical evaluation of evaporated liquid quantity. It characterized the relative water droplets sizes change during motion through the high-temperature gas area $\Delta R = (R_d - R_d^*)100/R_d$, [%], where R_d^* [mm] is droplet radius measured at the outlet (bottom) of high-temperature channel. Average radius was chosen as a characteristic droplet size due to the fact that the water droplet shape is close to the spherical [24-27] during the motion through high-temperature gas area. As a rule the droplet has close to ellipsoid shape. So we can talk only about conditional radius for objects with such configuration.

The droplets sizes (before and after high-temperature gas area) were determined by using the optical method [42-44]. Droplets in research area were illuminated (fig. 1) by the light pulse (6) repeatedly. The interference was observed between the reflected and refracted light by droplets. Droplet sizes [42-44] were determined according to the number of interference fringes observed on videograms. The average values of maximum diameters (from 6-10 values according to configuration) and characteristic values of condition radius R_d were calculated by IPI method [42-44] because of water droplets have the elliptic shape on videograms. Systematic inaccuracy of droplet size measurements were 0.001 mm.

Interferometric method for measuring droplets sizes IPI (also known as ILIDS) can be classified as field optical method for liquid and gas flows research. This method allows measuring the sizes of spherical droplets in the selected plane flow section [42-44]. The measurement of the spherical particle diameter by IPI method is carried out by analyzing the light intensity distribution scattered by such a particle. The measuring system includes a laser, its beam generates the light pulse, and a digital camera with a defocused lens. The camera records interference patterns directly from all drops, illuminated by light pulse, and the use of spherical and cylindrical lenses allow getting a droplet image *compressed* along one co-ordinate, preserving useful information – interference fringes, that significantly reduces the probability of overlapping droplets images. Then, the captured images are processed using special software. Instantaneous particles sizes distributions are determined by the distance between the stripes in the interference pattern formed by the light reflected and once refracted by droplet.

The PIV method was used for calculation of *tracer* particles evolution rate from the water droplet surface. These parameters characterized velocity of water vapor blowing in gas area and velocity of water evaporation [17, 18] as a consequence. According to PIV method the *tracer* particles were illuminated repeatedly in research area surface by the light pulse of laser. Particle images were recorded by a cross-correlation digital camera. Subsequent image processing allowed to calculate the particle displacement during the time between pulses of laser and to visualize a *two-component* field of *tracers* velocity [39-41]. These procedures were based on the cross-correlation algorithm intending the usage of fast Fourier transform method and a *correlation theorem* [39-41].

One of the main elements of the PIV method is to process the images obtained in the experiment [39-41]. When processing experiments videograms, the cross-correlation algorithm has been used (initial and final *tracers* positions are fixed on different frames). Each frame is divided into elementary measuring areas of fixed size. For each area the correlation function of particles shifts is calculated. The standard fast transform Fourier algorithm using the correlation theorem is being used. The maximum of the correlation function corresponds to the most probable particles shift in the given area. The velocity of the particles in a given unit area: $v = SD/\Delta t$ is determined, knowing the time delay between the laser flashes Δt, the scale factor S (calculated when calibrating the camera), and the most probable particles displacement D. The following procedure for each elementary area allows getting the *tracers* velocity field for an image [39-41].

Special utilities *top-hat* window [38] was applied to calculate the maximum of the correlation function and to decrease the quantity of random correlations associated with the effect of a *pair losses*. This allowed reducing the contribution of *tracers* to the correlation function that were located near (less than 1 pixel) the external borders of the video frame. The *instant* [38, 39] velocities of *tracers* were determined by the known time delays between the laser pulses and the most probable particle displacements (defined by the maximum of the correlation function) in the research area of video frames.

The filtration procedures were used during the *tracers* velocity calculation with specialized weight functions [39, 40]: *No-DC* (to constant component removal in the signal) and *Low-pass* (to increase the correlation peak width due to the cutoff of low frequencies of light shear and high frequencies of large proportions from correlation function spectrum). The elimination procedure was carried out of part of the *tracers* vectors obtained by *signal/noise* criterion [41]. Systematic inaccuracy of *tracers* velocity measurement in these conditions did not exceed 2%, according to the procedures [38-41].

Temperature of gas area (combustion products) was 1070 ± 30 K in channel (13). It was controlled by three chromel-alumel thermocouples (possible measurement of temperature range is 273-1373 K, the permissible variation is $\Delta = 3.3$ K) at different height levels (0.15 m, 0.5 m, 0.85 m) of cylinder. Initial temperature of water compositions was 298 K. It was controlled by two chromel-chapel thermocouples (possible measurement of temperature range is 233-573 K, the permissible variation is $\Delta = 2.5$ K).

In each experiment, the dispenser emitted one drop. Therefore, the measurements of sizes and velocities of movement have been carried out for the same drop. Measurements within the cylinder (13) can not be performed with satisfactory accuracy. This is due to vaporization and the difficulty in determining the interface *liquid – gas* in the system *drop-water vapors-the flame* (high-temperature combustion products). Therefore, droplet sizes and velocities of movement have been measured at the inlet and outlet of the high-temperature gas environment (13) in each experiment. Under identical initial conditions not less than ten experiments have been carried out. Then, the results averaging have been performed similar to experiments [25-27].

Results and discussion

The experiments carried out with water droplets contain in structure non-metallic (carbon) particles of different densities (from 1100-1900 kg/m^3). It was shown that their distribution in water droplets differed considerably at an equal relative mass concentration (γ_C) and sufficiently small (about 50 µm) particles size (L_m). Thus, carbon particles *deposition* processes in the droplets were observed for particles with significantly greater density (almost twice) relative of water density. Localization center of solid inclusions were formed near the droplet surface. There was the considerable deformation of the droplet surface and their subsequent destruction. It has been established that the detailed effects influence was weakened by reduction of particles density. For example, experimentally for solid particles (with density about 1200 kg/m^3, size $50 < L_m < 500$ µm and relative concentration $0 < \gamma_C < 1\%$) it was shown that the uniform distribution of solid particles is possible in water droplet with radius more than 1 mm.

Figure 2 shows typical videograms of water droplets (average radius $R_d = 3$ mm) with solid particles (carbon particles from 50-500 µm) at the inlet of high-temperature gas area.

It is visible, fig. 2(b) and (c), that particles with size $L_m > 200$ µm are chaotically situated relative to each other. Nevertheless they distributed rather uniform in water droplet. It can
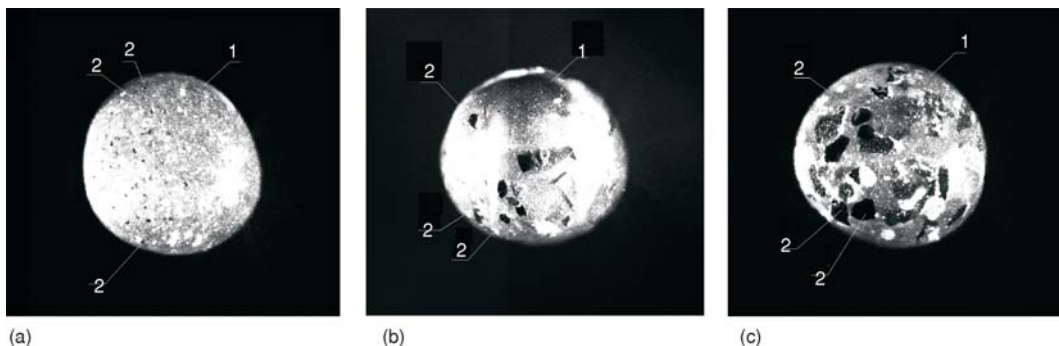

Figure 2. Videograms of water droplet ($R_d = 3$ mm) with the carbon particles in structure;
(a) $L_m = 50\text{-}70$ µm, (b) $L_m = 250\text{-}300$ µm, (c) $L_m = 450\text{-}500$ µm, at the inlet of the high-temperature gas area;
1 – droplet, 2 – carbon particles

be explained by carbon particles movement in water droplet due to convection. Solid particles with size $L_m \leq 70$ µm have close shape and uniform distribution in water droplet, fig. 2(a).

Droplets with configuration and distribution of solid particles similar to fig. 2 have been found at the outlet of the high-temperature gas area. However, this feature remains in case of $L_m < 400$ µm. Water droplet with solid particles ($L_m > 400$ µm and $\gamma_C = 0$-1%) is significantly deformed in the high-temperature gas area. The most typical configurations of such droplet were shown in fig. 3. Changing of droplet configuration had a random nature (fig. 3). It can be explained by significantly heterogeneous droplet structure. Existence of solid particles leads to a reduction of viscosity in the *water – carbon particles* structure. Besides, the liquid surface tension force decreases on the droplet surface with carbon particles inclusions. Carbon particles are heated faster than water (due to the relevant thermal properties). This leads to vaporization enhancement around particles within a droplet. Pressure changes around each particle in the droplet. This cause a deformation enhancement of droplet layers, as a heterogeneous structure. The influence of selected effects is enhanced as inclusions sizes increasing. In case of $L_m < 400$ µm a good experimental result repeatability has been established both in qualitative (droplet configuration) and quantitative (ΔR) indicators.
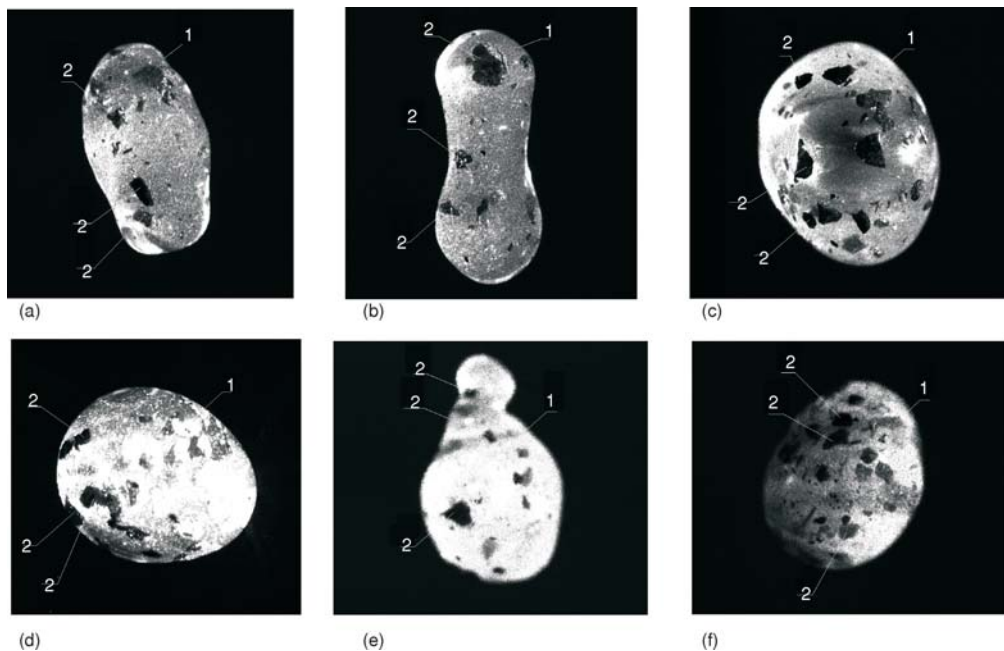

Figure 3. Videograms of water droplet (the initial radius $R_d = 3$ mm) with the carbon particles in structure ($L_m = 450$-500 µm) at the outlet of the high-temperature gas area; (a)-(f) is the most typical configurations);

Figure 4 shows two curves characterizing the dependences of parameter ΔR on initial radius (R_d) of water droplet without solid particles and include carbon particles in structure ($\gamma_C = 0.8\%$, $L_m = 250$-300 µm). Obtained dependences proves evaporation enhancement as a result of higher rate heat and mass transfer processes at warming water droplet with solid particles. The determined feature is more expressed (fig. 4) for droplet with a smaller size and other equal conditions (concentration and size of solid particles).

Tracers velocity near the droplet surface (V_v = 0.07-0.18 m/s) have been calculated by the PIV method analyze of water droplet videograms. Water vapor density ρ_v under concerned conditions did not exceed 3 kg/m^3 [16-18]. According to equation $W_e = V_v \rho_v$ [17, 18], the mass velocity of water evaporation W_e= = 0.21-0.54 kg/m^{2}s. It has been established that the maximum evaporation velocity near the front of the water droplet motion. Value of W_e significantly lower (25% less) in the water droplet trace. The reason for this was not only the combustion product temperature decreases

Figure 4. Dependence of ΔR parameter on initial droplet radius R_d

in the droplet trace (as a consequence at the *liquid – gas* border) but also the vapor film formation between the droplet and the high-temperature gas area. This layer looks as a buffer zone which decreased the heat flux to the water droplet at 20-30%. The received results (in particular, velocity of water evaporation W_e) are in good agreement with the main conclusions of numerical investigations of heat and mass transfer processes and phase transitions at the system *water droplet-high-temperature gases* [16-18].

Figure 5 shows the dependence of ΔR parameter on the relative mass concentration of carbon particles in water droplet (γ_C) with initial radius R_d = 3 mm (solid particles size L_m varied in the range 250-300 µm).

The velocity of change of evaporated droplet size and weight have been established during the analysis of parameter ΔR and characteristic time of water droplet motion through the high-temperature channel (fig. 1). The last one characterized the mass velocity of vaporization, that reached the value of W_e = 0.3 kg/m^{2}s. The W_e reduced to 30-35% in case of smaller concentration (γ_C < 1%) of solid particles in water droplet structure. The obtained result proves a good correlation of W_e values calculated by the PIV and IPI methods.

Figure 5. Dependence of ΔR parameter on relative mass concentration of carbon particles γ_C at L_m = 250-300 µm for droplets with R_d = 3 mm

It has been established that the higher γ_C the more parameter ΔR during water droplet motion through high-temperature gas area (fig. 5). As a consequence the quantity of the evaporated liquid and the rate of vaporization increased considerably. This effect can be explained by the fact that the thermal conductivity of heterogeneous *water droplet – solid particles* system raised (in several times) even at rater low increasing of γ_C (from 0-1%). It leaded to considerably reduction of the time period necessary for near-surface layer of the water droplet warming and its follow endothermal phase transformation.

Thermal conduction, thermal convection and radiative heat transfer took place at the water droplet warming during its motion through the high-temperature gas area. According to experimental results solid particles motion in water droplet and its *luminescence* was registered. Carbon particles absorbed significantly more heat due to radiative transfer from combustion products in comparison with water droplet. The heat accumulated in *water droplet – solid parti-*
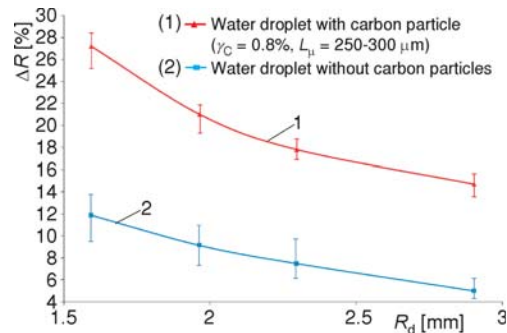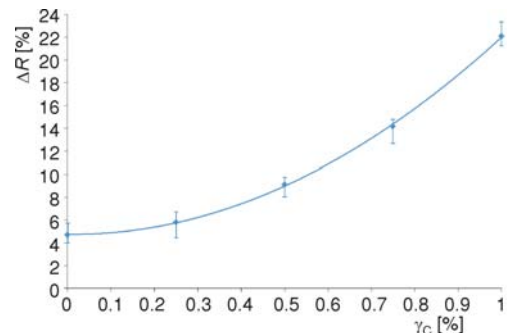
cles system increased. The local phase transformation areas were formed near the border of solid particles. It led to the movement of both carbon particles and liquid layers inside droplet (the thermal convection was realized).

After the analysis of experimental videograms we make a conclusion about evaporation enhancement due to the great values of radiative heat flux from the high-temperature gas area to the water droplet with solid particles in comparison with water droplet without carbon particles. It can be explained by the fact that heat flux from the gas area to carbon particles significantly (about 5-6 times) higher than the heat flux to water in other equal parameters. As a result, solid particles temperature and respectively water droplet temperature could reach much higher value compared to the homogeneous water droplet even in case of low concentration of particles ($\gamma_C = 0$-1%). Water evaporation occurred near the each solid particles. Evaporation velocity essential exceeded the analog parameter for homogeneous water droplet. Intensive evaporation led to vapor layer formation near the solid particles and the subsequent dispersion of *heterogeneous* droplet. This effect might be the reason of *heterogeneous* droplet size reduction in comparison with homogeneous one in identical experimental conditions.

The influence of analyzed effects on intensity of liquid warming significantly grew up at increasing of solid particles size in water droplet. Figure 6 shows the dependence of parameter ΔR on characteristic size L_m of carbon particles for water droplet with radius $R_d = 3$ mm. It is visible that $\Delta R = 6.9\%$ for particles with size $L_m = 50$-70 µm, $\Delta R = 7.1\%$ for particles with size $L_m = 250$-300 µm, and $\Delta R = 14.1\%$ for particles with size $L_m = 450$-500 µm.

Also the experiments have been conducted to establish the limiting values of solid particles size in water droplet, which led to its destruction. The droplet sizes were varied (from tens to hundreds of micrometers) according to the *finely atomized* water structure [11-13]. It has been revealed that the limiting values of L_m were 60-70 µm for droplets with radius $R_d = 0.1$-0.15 mm during its motion through high-temperature gas channel with a length of 1 m, for example. The obtained result shows that the relatively large solid particle in the droplet enhance its warming, deformation, and destruction more significantly as compared with several smaller particles in droplet structure. According to experimental research results water droplet destruction during its motion in the high-temperature gas area is possible in case of big size of solid particle (about 50-60% of the droplet size). The established features were in good agreement with the basic concepts of the modern theory of gas-vapor-droplet flows at the phase transitions [45-52]. Developed experimental technique can significantly extend the representation of the investigations [45-52].
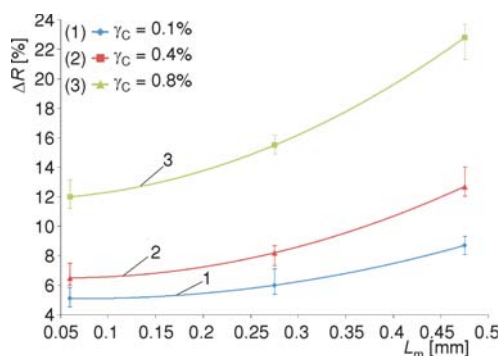

Figure 6. Dependence of ΔR parameter on the size of carbon particles L_m for droplets with $R_d = 3$ mm

The analyzed effects can be used for evaporation enhancement of water pulverized by firefighting aircraft above the combustion area. For example, the substantial decomposition of water droplets is not necessary even at relatively small concentration of solid particles (less than 1%) in droplet structure. Only the batch droplets supply is expedient. Destruction of moving water droplets is possible due to the thermal conduction, thermal convection and radiation transfer. As a consequence the cloud of water droplets forms. Its efficiency during firefighting process was proved by the numerical research results [1-13] in comparison with firefighting by monolithic water flow.

The experimental research results allow concluding about important role of water quality supplied in the combustion area. According to modern firefighting techniques used by firefighting aircraft the water which is taken away from a reservoir, can have different solid particles in structure. Its concentration may substantially exceed 1%. In this case, it is very difficult to predict the consequences, control the process of firefighting and improve its efficiency. Therefore, it is necessary to pay attention to the water quality.

Experimental research results can be used to develop the extinguishing technologies both as forest and large urban fires. Obtained dependences between sizes of water droplet and solid particles can be used for development of water spray equipment for effective firefighting.

Conclusions

In this study we determined that the solid non-metallic particles in a large ($R_d =$ = 1-5 mm) water droplets significantly enhance evaporation process during the water droplet motion through high-temperature gas area. It has been established that the higher mass concentration and size of solid particles in a water droplet the higher (by several times) evaporation velocity of liquid. Obtained results illustrate important role of solid particles in water droplet for increasing efficiency of firefighting process by sprayed water.

Acknowledgment

Nomenclature

D – movement of particles in the elementary area, [pix]
L_m – size of solid carbon particles, [μm]
R_d – droplet radius measured at the inlet (top) of high-temperature channel, [mm]
R_d^* – droplet radius measured at the outlet (bottom) of high-temperature channel, [mm]
ΔR – the parameter characterized the relative water droplets sizes change during motion through the – high-temperature gas area, [%]
S – scale coefficient, [mm/pix]
Δt – time delay between the laser flashes, [ms]
V_v – *tracers* velocity near the droplet surface, [ms^{-1}]
W_e – the mass velocity of water evaporation, [kgm^{-2}s^{-1}]

Greek symbols

γ_C – the relative mass concentration of carbon particles in water droplets, [%]
Δ – the permissible variation of temperature measurement, [K]
ρ_v – water vapor density, [kgm^{-3}]
v – velocity of particles in the elementary area, [ms^{-1}]

Acronyms

ILIDS – interferometric laser imaging for droplet sizing
IPI – interferometric particle imaging
PIV – particle image velocimetry

References

[1] Wighus, R., Water Mist Fire Suppression Technology – Status and Gaps in Knowledge, *Proceedings*, International Water Mist Conference, Vienna, Austria, 2001, pp. 1-26
[2] Karpov, A. I., *et al*., Numerical Modeling of the Effect of Fine Water Mist on the Small Scale Flame Spreading over Solid Combustibles, *Proceedings*, 8th International Symposium Fire Safety Science, Beijin, China, 2005, pp. 753-764
[3] Xiao, X. K., *et al.*, On the Behavior of Flame Expansion in Pool Fire Extinguishment with Steam Jet, *Journal of Fire Sciences, 29* (2011), 4, pp. 339-360

[4]   Qimiao, X., *et al*., The Effect of Uncertain Parameters on Evacuation Time in Commercial Buildings, *Journal of Fire Sciences, 30* (2012), 1, pp. 55-67

[5]   Na, M., *et al*., Full-Scale Experimental Study on Fire Suppression Performance of a Designed Water Mist System for Rescue Station of Long Railway Tunnel, *Journal of Fire Sciences, 30* (2012), 1, pp. 138-157

[6]   Yao, B., Cong, B. H., Experimental Study of Suppressing Poly (Methyl Methacrylate) Fires Using Water Mists, *Fire Safety Journal, 47* (2012), Jan., pp. 32-39

[7]   Korobeinichev, O. P., *et al*., Fire Suppression by Low-Volatile Chemically Active Fire Suppressants Using Aerosol Technology, *Fire Safety Journal, 51* (2012), July, pp. 102-109

[8]   Tang, Z., *et al*., Experimental Study of the Downward Displacement of Fire-Induced Smoke by Water Sprays, *Fire Safety Journal, 55* (2013), Jan., pp. 35-49

[9]   Abbud-Madrid, A., *et al.*, On the Effectiveness of Carbon Dioxide, Nitrogen and Water Mist for the Suppression and Extinction of Spacecraft Fires, *Proceedings*, Suppression and Detection Research and Applications Conference, Orlando, Fla., USA, 2007

[10] Carriere, T., *et al.*, Fire Suppression Test Using a Handheld Water Mist Extinguisher Designed for the International Space Station, *Proceedings*, 42nd International Conference on Environmental Systems, San Diego., Cal., USA, 2012

[11] Rodriquez, B., Young, G., Development of the International Space Station Fine Water Mist Portable Fire Extinguisher, *Proceedings*, 43rd International Conference on Environmental Systems, Vail., Col., USA, 2013, pp. 1-8

[12] Macindoe, L., Leonard, J., Moisture Content in Timber Decking Exposed to Bushfire Weather Conditions, *Fire and Material, 36* (2012),1, pp. 49-61

[13] McAllister, S., Critical Mass Flux for Flaming Ignition of Wet Wood, *Fire Safety Journal, 61* (2013), Oct., pp. 200-206

[14] Nikolopoulos, N., *et al*., A Numerical Investigation of the Evaporation Process of a Liquid Droplet Impinging onto a Hot Substrate, *International Journal of Heat and Mass Transfer, 50* (2007),1-2, pp. 303-319

[15] Misyura, S. Y., *et al*., The Behavior of Water Droplets on the Heated Surface, *International Journal of Heat and Mass Transfer, 55* (2012), 23-24, pp. 6609-6617

[16] Vysokomornaya, O. V., *et al*., Heat and Mass Transfer in the Process of Movement of Water Drops in a High-Temperature Gas Medium, *Journal of Engineering Physics and Thermophysics, 86* (2013), 1, pp. 62-68

[17] Strizhak, P. A., Influence of Droplet Distribution in a "Water Slug" on the Temperature and Concentration of Combustion Products in its Wake, *Journal of Engineering Physics and Thermophysics, 86* (2013), 4, pp. 895-904

[18] Kuznetsov, G. V., Strizhak, P. A., Numerical Investigation of the Influence of Convection in a Mixture of Combustion Products on the Integral Characteristics of the Evaporation of a Finely Atomized Water Drop, *Journal of Engineering Physics and Thermophysics, 87* (2014), 1, pp. 103-111

[19] Xiangyang, Z., *et al*., Spray Characterization Measurements of a Pendent Fire Sprinkler, *Fire Safety Journal, 54* (2012), Nov., pp. 36-48

[20] Gupta, M., *et al*., Experimental Evaluation of Fire Suppression Characteristics of Twin Fluid Water Mist System, *Fire Safety Journal, 54* (2012), Nov., pp. 130-142

[21] Forsth, M., Moller, K., Enhanced Absorption of Fire Induced Heat Radiation in Liquid Droplets, *Fire Safety Journal, 55* (2013), Jan., pp. 182-196

[22] Yoshida, A., *et al.*, Experimental Study of Suppressing Effect of Fine Water Proplets on Propane/Air Premixed Flames Stabilized in the Stagnation Flowfield, *Fire Safety Journal, 58* (2013), May, pp. 84-91

[23] Joseph, P., *et al*., A Comparative Study of the Effects of Chemical Additives on the Suppression Efficiency of Water Mist, *Fire Safety Journal, 58* (2013), May, pp. 221-225

[24] Volkov, R. S., *et al*., Experimental Study of the Change in the Mass of Water Droplets in their Motion through High-Temperature Combustion Products, *Journal of Engineering Physics and Thermophysics, 86* (2013), 6, pp. 1413-1418

[25] Volkov, R. S., *et al*., Influence of the Initial Parameters of Spray Water on Its Motion through a Counter Flow of High Temperature Gases, *Technical Physics, 59* (2014), 7, pp. 959-967

[26] Kuznetsov, G. V., Strizhak, P. A., Evaporation of Single Droplets and Dispersed Liquid Flow in Motion through High Temperature Combustion Products, *High Temperature, 52* (2014), 4, pp. 568-575

[27] Volkov, R. S., et al., Evaporation of Two Liquid Droplets Moving Sequentially through High-Temperature Combustion Products, *Thermophysics and Aeromechanics, 21* (2014), 2, pp. 255-258

[28] Steinhaus, T., *et al.*, Large-Scale Pool Fires, *Thermal Science, 11* (2007), 1, pp. 101-118
[29] Stevanović, Ž., *et al.*, Numerical Simulation of Fire Spread in Terminal 2 of Belgrade Airport, *Thermal Science, 11* (2007), 1, pp. 251-258
[30] Banjac, M. J., Nikolić, B. M., Computational Study of Smoke Flow Control in Garage Fires and Optimisation of the Ventilation System, *Thermal Science, 13* (2009), 1, pp. 69-78
[31] Stefanov, S. B., *et al.*, Ecological Modeling of Pollutants in Accidental Fire at the Landfill Waste, *Thermal Science, 17* (2013), 4, pp. 903-913
[32] McAllister, S., *et al.*, Piloted Ignition of Live Forest Fuels, *Fire Safety Journal, 51* (2012), July, pp. 133-142
[33] Madrigal, J., et al., A New Bench-Scale Methodology for Evaluating the Flammability of Live Forest Fuels, *Journal of Fire Sciences, 31* (2013), 2, pp. 131-142
[34] Thompson, M. P., *et al.*, Airtankers and Wildfire Management in the US Forest Service: Examining Data Availability and Exploring Usage and Cost Trends, *International Journal of Wildland Fire, 22* (2012), 2, pp. 223-233
[35] Okamoto, K., *et al.*, Evaporation and Diffusion Behavior of Fuel Mixtures of Gasoline and Kerosene, *Fire Safety Journal, 49* (2012), Apr., pp. 47-61
[36] Sudheer, S., *et al.*, Physical Experiments and Fire Dynamics Simulator Simulations on Gasoline Pool Fires, *Journal of Fire Sciences, 31* (2013), 4, pp. 309-329
[37] Ding, C., *et al.*, Experimental Study and Hazard Analysis on the Flash Point of Flammable Liquids at High Altitudes, *Journal of Fire Sciences, 31* (2013), 4, pp. 469-477
[38] Keane, R. D., Adrian, R. J., Theory of Cross-Correlation Analysis of PIV Images, *Applied Scientific Research, 49* (1992), 3, pp. 191-215
[39] Westerweel, J., Fundamentals of Digital Particle Image Velocimetry, *Measurement Science and Technology, 8* (1997), 12, pp. 1379-1392
[40] Foucaut, J. M., Stanislas, M., Some Considerations on the Accuracy and Frequency Response of Some Derivative Filters Applied to Particle Image Velocimetry Vector Fields, *Measurement Science and Technology, 13* (2002), 7, pp. 1058-1071
[41] Willert, C., Assessment of Camera Models for Use in Planar Velocimetry Calibration, *Experiments in Fluids, 41* (2006), 1, pp. 135-143
[42] Glantschnig, W. J., Chen, S., Light Scattering from Water Droplets in the Geometrical Optics Approximation, *Applied Optics, 20* (1981), 14, pp. 2499-2509
[43] Konig, G., *et al.*, A New Light-Scattering Technique to Measure the Diameter of Periodically Generated Moving Droplets, *J. of Aerosol Sci, 17* (1986), 2, pp. 157-167
[44] Kawaguchi, T., *et al.*, Size Measurements of Droplets and Bubbles by Advanced Interferometric Laser Imaging Technique, *Meas Sci and Technol, 13* (2002), 3, pp. 308-316
[45] Sazhin, S. S., *et al.*, Models for Drop Transient Heating: Effects on Drop Evaporation, Ignition, and Break-up, *International Journal of Thermal Sciences, 44* (2005), 7, pp. 610-622
[46] Ebrahimian, V., Gorji-Bandpy, M., Two-Dimensional Modeling of Water Spray Cooling in Superheated Steam, *Thermal Science, 12* (2008), 1, pp. 79-88
[47] Kryukov, A. P., Levashov, V. Yu., About Evaporation-Condensation Coefficients on the Vapor-Liquid Interface of High Thermal Conductivity Matters, *International Journal of Heat and Mass Transfer, 54* (2011), 13-14, pp. 3042-3048
[48] Han, Y., *et al.*, The Effect of Liquid Film Evaporation on Flow Boiling Heat Transfer in a Micro Tube, *International Journal of Heat and Mass Transfer, 55* (2012), 4, pp. 547-555
[49] Ahmadikia, H., *et al.*, Simultaneous Effects of Water Spray and Crosswind on Performance of Natural Draft Dry Cooling Tower, *Thermal Science, 17* (2013), 2, pp. 443-455
[50] Shanthanu, S., *et al.*, Transient Evaporation of Moving Water Droplets in Steam - Hydrogen - Air Environment, *International Journal of Heat and Mass Transfer, 64* (2013), Sep., pp. 536-546
[51] Autee, A., *et al.*, Experimental Study on Two-Phase Pressure Drop of Air-Water in Small Diameter Tubes at Horizontal Orientation, *Thermal Science, 18* (2014), 2, pp. 521-532
[52] Glushkov, D. O., *et al.*, Numerical Investigation of Water Droplets Shape Influence on Mathematical Modeling Results of its Evaporation in Motion through a High-Temperature Gas, *Mathematical Problems in Engineering, 2014* (2014), ID 920480